UTILIZATION FACTOR IMPROVMENT OF A GRID CONNECTED PHOTOVOLTAIC SYSTEM INCORPORATING HERIC TRANSFORMERLESS INVERTER

Sherif A. ZAID

Electrical Power and Machines Department, Faculty of Engineering, Cairo University, Egypt
Email: sherifzaid3@yahoo.com

Abstract:- *For the grid connected Photovoltaic (PV) systems, HERIC transformerless inverter is considered one of the most efficient, reliable, and nearly leakage free inverters. Unfortunately, this inverter typically draws a discontinuous current from the PV. However, continuous PV current is required to ensure Maximum Power Point (MPP) operation. Hence, MPP operation of the HERIC inverter is not a clear issue. Also, the utilization factor (Kpv) of the PV drops to small value (≅ 50%), which in turn increases the size and cost of the PV system. In this paper, a boost converter is inserted between the HERIC inverter and PV then the system is modeled, analyzed, and compared to the traditional topology. Simulations for the traditional HERIC inverter and the proposed system are done to validate the idea and the analyses.*

Key words: Inverter, transformerless, PV, HERIC, MATLAB.

1. Introduction

Photovoltaic system is one of the most promising renewable energy systems as it is clean and reliable. It is no longer more expensive than traditional fossil fuels in many parts of the world[1]. Canadian Solar, one of the big three global solar PV manufacturers, delivered a detailed update of its outlook Fig. 1 [2], including some interesting forecasts on the future of solar PV costs. It says that the cost of solar PV modules will likely fall 25% in the next three years, from 0.47 $/w by the end of 2014, to 0.36$/w by the end of 2017.This explains the large spread installations and the worldwide applications of the PV systems. PV installations are no longer isolated from the grid but connected to it, seeking to become part of the electricity generation mix. The power generation of grid connected PV system is increasing continuously all over the world, reaching values of hundreds of mega-watts [3].Thus, making these systems a crucial part of the future electric energy systems and smart grids. Nowadays, most of the PV systems are dedicated to the residential market with typical system sizes around 2–10kW[4]. Traditional residential PV systems included a single phase inverter with a transformer between the inverter and the grid. The transformer is useful for galvanic isolation thus providing personal safety. Furthermore, it ensures that no direct current, which could saturate the distribution transformer, is injected into the grid. Finally, it can be utilized to increase the inverter output voltage level[5]. However, transformers make the system heavy, increase the size, increase the cost of the PV system, and reduce its efficiency. Therefore, the transformerless PV grid connected inverters are widely installed in the low power PV generation systems[6].

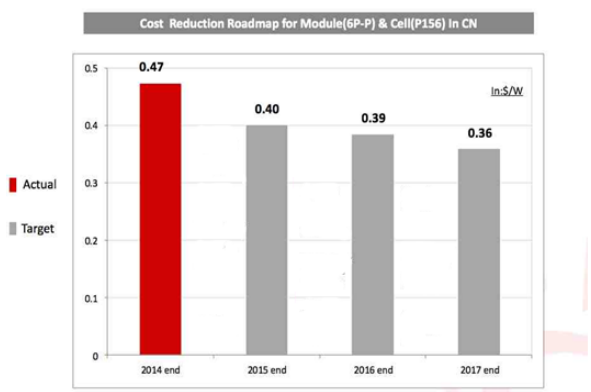

Fig. 1 Cost reduction road map of PV modules, by Canadian Solar Company[2].

Unfortunately, when the transformer is removed, varying common mode (CM) voltage that produces leakage current may appear in the system which

flows through the parasitic capacitances between the PV panels and the ground [7]. Moreover, leakage currents lead to serious safety and radiated interference issues [7]. Therefore, they must be limited within a reasonable range [6-8]. In order to remove leakage currents, the CM voltage must be kept constant or only varied at low frequency, such as 50Hz/60Hz [6].

A traditional method to solve this problem is to apply the full-bridge inverter with the bipolar sinusoidal pulse width modulation (SPWM). The CM voltage of this inverter is kept constant during all operating modes. Thus, it features excellent leakage currents characteristic. However, terminal voltage step is twice of the DC-link voltage, which results in large Electro Magnetic Interference (EMI) noise, high Total Harmonic Distortion (THD), large switching losses, and low conversion efficiency[9,10]. Also, the conversion efficiency is greatly reduced due to the fact that there is a reverse power flow associated with this method[11,12].The full-bridge inverters with unipolar SPWM control are attractive owing to the excellent THD current, smaller inductor current ripple, lower EMI noise, and higher conversion efficiency. The main drawback is the fact that it generates a varying CM voltage of amplitude equals half the DC-link voltage, at the switching frequency, which leads to high leakage currents [7].

Recently, various topologies have been developed and researched to solve the problem of keeping the leakage current lower the standard regulation values [13]. These topologies tries to gain all advantages given by the unipolar SPWM, but still having the CM voltage as in the case of bipolar SPWM. One of the most efficient and perfect inverters used for grid connected PV systems is the High Efficiency and Reliable Inverter Concept (HERIC) [14]. This topology has been implemented in some commercial inverters, especially those from Sunway's converter [12]. It really has high efficiency and eliminates the leakage current effectively.

Unfortunately, there are three problems regarding the power flow from the PV to the grid through the HERIC topology. The first problem, is that the HERIC topology, like all the recently developed topologies, are based on disconnecting the PV from the grid during the zero states or freewheeling states. Therefore the utilization factor (K_{pv}) of the PV drops to small values (≅ 50%); as will be explained. This factor should be raised to avoid over size and cost of the PV system. Typical value of K_{pv} is around 98%[15].

The second important problem is that the inverters must guarantee that the PV module(s) is operated at the MPP, which is the operating condition where the most energy is captured. This is accomplished with a MPP tracker (MPPT). This involves that the PV current, for a certain insolation level, must be constant at the value of the MPP conditions. However, this is not the case with the ordinary galvanic isolation techniques.

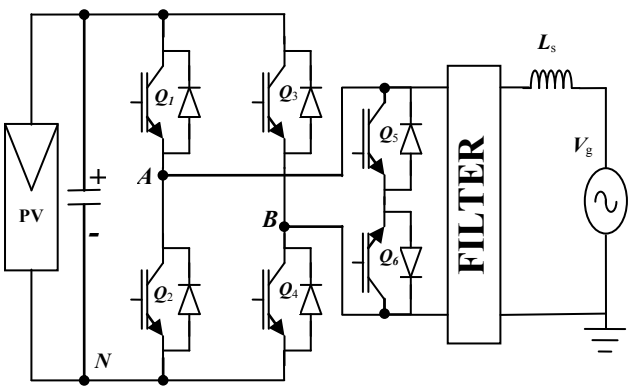

Fig. 2 HERIC inverter circuit.

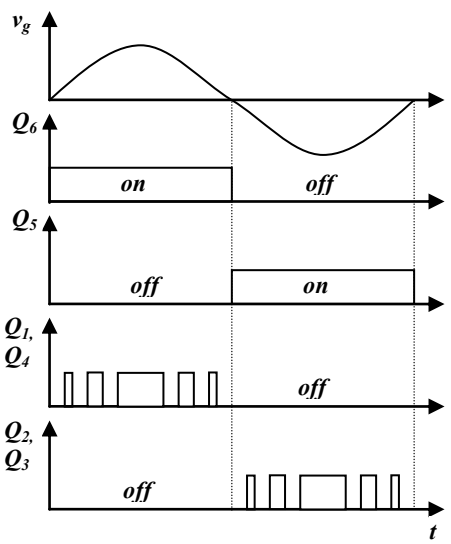

Fig. 3 HERIC inverter switches gate signals

The third problem is that the power flow to the grid is time varying, while the power of the PV

panel must be constant for maximizing energy harvest, which results in an instantaneous input

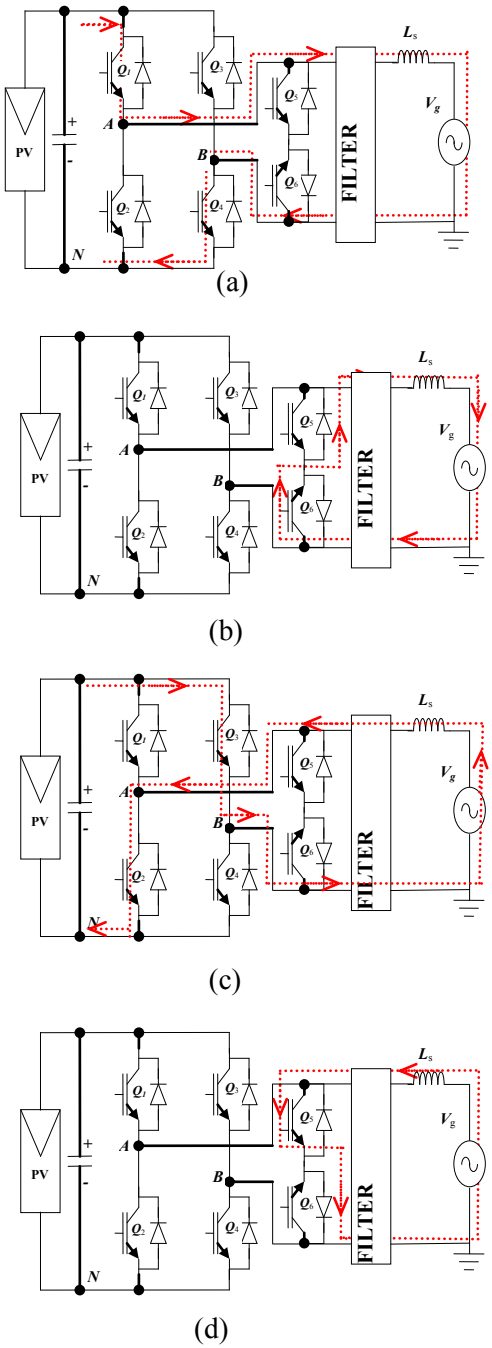

Fig. 4 Modes of operation of HERIC inverter (a) mode 1, (b) mode 2,(c) mode 3, (d) mode 4.

Power mismatch with the output instantaneous AC power to the grid. Therefore, energy storage elements must be placed between the input and output to balance (decouple the unbalance) the different instantaneous input and output powers [16]. Usually, a capacitor is used to serve as a power decoupling element. However, the lifetime, the space, and complexity of the system increased that conflicts with the requirements of operators and consumers. Some researchers have explored various ways to reduce the size of the required capacitance [16-17]. In order to elevate the PV captured energy and the K_{pv} factor, a boost converter is added to the HERIC inverter.

In this paper, analyses of the HERIC inverter are carried out to derive the K_{pv} factor. Simulations for the traditional HERIC inverter and the proposed system are done to validate the idea and the analyses.

2. HERIC Inverter Operation

The advanced HERIC inverter is simply formed of the traditional H-bridge while its load terminals are shunted by an AC switch as shown in Fig.2.This switch consists of two back to back transistors Q5&Q6.Each transistor has an antiparallel diode. Transistors are opposite in operation and operating at the grid frequency. The functions of the AC switch are to bypass the current during the zero state periods and decouple the inverter from the grid. Assuming that the grid current is of unity power factor, the inverter operation is as follows:

The gate signals used to drive the inverter switches are shown in Fig.3.

- The signals of Q5&Q6 are square waves synchronized to the grid voltage, such that Q6is on at positive half cycle. While Q5 is on at the negative half cycle.
- The signals of Q1&Q4 of the H-bridge are switched simultaneously, with SPWM, at the switching frequency (only operate at the positive half cycle).
- The signals of Q2&Q3 of the H-bridge are switched simultaneously, with SPWM, at the switching frequency (only operate at the negative half cycle).

This results in four operating modes, two modes in each half cycle.

Mode(1)only Q1&Q4&Q6 are on

In this case, the current flow from PV to the grid throughQ1&Q4, while Q6 does not carry current as shown in Fig. 4-a. It is called active state mode.

Mode(2) only Q6 is on

In this case, the grid current freewheels through Q6 and D5, while the PV is disconnected from the grid as shown in Fig. 4-b. It is called zero state mode.

Mode(3) only Q2&Q3&Q5 are on

In this case, the current flow from PV to the grid through Q2&Q3, while Q5 does not carry current as shown in Fig. 4-c. It is called active state mode.

Mode(4) only Q5 is on

In this case, the grid current freewheels through Q5 and D6, while the PV is disconnected from the grid as shown in Fig. 4-d. It is called zero state mode.

The on state losses and switching losses of this topology is less than that recently introduced topologies[10].

Also, during the zero state mode, the reactive grid current is kept away from the PV.This has a strong impact on the overall system efficiency and systems design. A further advantage of this topology is the low leakage current, as the common mode voltage is constant[11].

2.1 Calculation of PV utilization factor with HERIC inverter

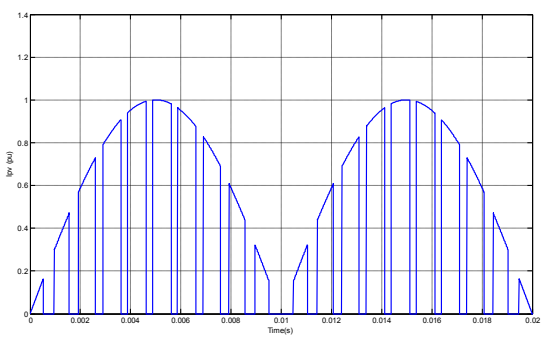

Fig. 5 Typical PV current of HERIC inverter.

As shown in Fig. 5, the current delivered by the PV is not continuous. Hence, the K_{pv} factor is worse and the MPP tracking isa vague issue, when used with this loading conditions. Now, we will try to calculate the $\boldsymbol{K_{pv}}$ factor assuming that the PV current $\boldsymbol{i_{pv}}$as in case of typical shape shown in Fig.5. The $\boldsymbol{K_{pv}}$ factor is defined as the average generated power divided by the theoretical MPP power $\boldsymbol{P_{MPP}}$:

$$K_{PV} = \frac{P_{PV}}{P_{MPP}} \qquad (1)$$

Where; $\boldsymbol{P_{PV}}$ = the average actual PV power and $\boldsymbol{P_{MPP}}$ = the maximum PV power for a given insolation.

The value of $\boldsymbol{P_{PV}}$is the average of the instantaneous PV voltage $\boldsymbol{v_{pv}}$ and current $\boldsymbol{i_{pv}}$ product:

$$P_{PV} = 2f_g \int_0^{\frac{0.5}{f_g}} v_{pv} * i_{pv} dt \qquad (2)$$

For simplicity, assuming that $\boldsymbol{v_{pv}}$ has constant value ($\mathbf{V_{MPP}}$) at MPP condition. Hence, the average actual PV power can be written as:

$$P_{PV} = 2f_g * \mathrm{V_{MPP}} \int_0^{\frac{0.5}{f_g}} i_{pv} dt \qquad (3)$$

According to Fig. 5, $\boldsymbol{i_{pv}}$ is a full wave rectified sine wave at the grid frequency and modulated with the PWM of the HERIC inverter. The amplitude of $\boldsymbol{i_{pv}}$ equals to the delivered peak current supplied to the grid. That current is usually delivered at unity power factor, as we assume here. With reference to the method of regular sampling of sinusoidal PWM, the duty ratio $\boldsymbol{D_n}$ of the $\boldsymbol{n}$ switching cycle is given by [18]:

$$D_n = m \sin(2\pi \frac{f_g}{f_s} n) \qquad (4)$$

Where; $\boldsymbol{n}$ = order of the switching cycle, $\boldsymbol{f_s}$ = switching frequency, $\boldsymbol{f_g}$ = grid frequency, and $\boldsymbol{m}$ = modulation index. Hence, the on time of the active state current is $\boldsymbol{T_s D_n}$, while the on time of the zero state current is $\boldsymbol{T_s(1\text{-}D_n)}$. Assuming that the current is constant during the active state current at:

$$i_{pv}(n) = I_m \sin(2\pi \frac{f_g}{f_s} n) \qquad (5)$$

Where; $\mathbf{I_m}$ = the peak current, $1 \le \boldsymbol{n} \le \boldsymbol{m_f}/2$, and $\boldsymbol{m_f = f_s / f_g}$ is the frequency modulation ratio. Substitute (5) into (2), the integration sign is transformed into the summation sign as:

$$\mathrm{P_{PV}} = 2f_g \sum_{n=1}^{m_f/2} \mathrm{I_m V_{MPP}} \sin(\frac{2\pi n}{m_f}) * D_n T_s \qquad (6)$$

Substitute (4) into (6);

$$\mathrm{P_{PV}} = \frac{2}{m_f} \sum_{n=1}^{m_f/2} m \mathrm{I_m V_{MPP}} \sin^2(\frac{2\pi n}{m_f}) \qquad (7)$$

Let $\mathbf{I_m} = \mathbf{I_{MPP}}$ then substitute (7) into (1);

$$K_{PV} = \frac{2m}{m_f}\sum_{n=1}^{m_f/2}\sin^2\left(\frac{2\pi n}{m_f}\right) \qquad (8)$$

In trying to plot equation (8), it was found that $\boldsymbol{K_{pv}} = 0.5\boldsymbol{m}$ for all values of $\boldsymbol{m_f}$. Therefore, we investigate that by manipulating equation (8), $\boldsymbol{K_{pv}}$ can be written as following:

$$K_{PV} = \frac{0.5m}{m_f}\left(m_f - \sum_{n=1}^{m_f/2}\cos\left(\frac{4\pi n}{m_f}\right)\right) \qquad (9)$$

For unipolar PWM, $\boldsymbol{m_f}$ must be an even integer [9]. Therefore, active current states are distributed symmetrically around the zero point of the cosine function. That in turn forces the summation part of (9) to be zero. Hence,

$$\boldsymbol{K_{pv}} = 0.5\boldsymbol{m} \qquad (10)$$

Equation (10) shows that $\boldsymbol{K_{pv}}$ is as low as 0.5, if $\boldsymbol{m}$ =1. These analyses will be supported by the following simulations.

3. Improved HERIC Inverter

The It has been verified, from the previous paragraphs, that the conventional HERIC inverter draws discontinuous current from the PV. That issue degrades $\boldsymbol{K_{pv}}$ and does not assure the condition of MPP. These problems can be elevated by inserting a boost converter between the PV and the HERIC inverter. The boost converter is designed to operate in continuous conduction mode with very small current ripple 1%. Hence, the boost source current which is the PV current is constant. The boost converter is controlled so as to force the PV at the MPP condition.

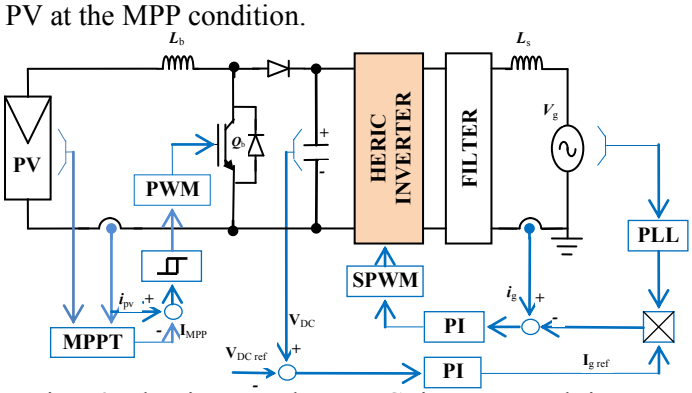

Fig. 6 The improved HERIC inverter and its controller.

Another important function of the boost converter is the ability to capture small generated power from the PV by boosting $\boldsymbol{V_{pv}}$. The improved HERIC inverter system is shown in Fig. 6. To extract maximum power from the PV array, mechanical and electrical techniques are applied. Mechanical techniques are based essentially on the optimization of the PV array space angles so as to maximize the incident solar energy. However, electrical techniques are based essentially on the optimization of the PV array load in such a way to generate most of the incident solar energy [15]. In this paper, the interest is on the electrical MPP technique. The objectives of the controller are to maintain MPP condition of the PV, adjust the DC link voltage, and control the grid current to be sinusoidal of unity power factor. The voltage and current of the PV panel is fed to the MPPT loop that generates the reference current of the boost converter current controller .The reference value of V_{DC} is adjusted to a typical value of 400V. The HERIC inverter controller is the same as the conventional except for the value of $\boldsymbol{I_{g\ ref}}$ that is generated by the PI controller as shown in Fig.6.The phase locked loop (PLL) synchronizes PV system with the grid; in a manner such that unity power factor is guaranteed.

3.1 The PV utilization factor with improved HERIC inverter

In calculating $\boldsymbol{K_{pv}}$ for the improved HERIC system, shown in Fig.6, the shape and value of $\boldsymbol{i_{pv}}$ have great importance. It was found that $\boldsymbol{i_{pv}}$ has small ripples. These ripples must be up to 2–4% of the MPP condition so as not to compromise $\boldsymbol{K_{pv}}$ significantly [19]. If the boost converter is designed such that the ripples are so small, $\boldsymbol{i_{pv}}$ can be considered constant. If the set point of the controller is adjusted to be $\mathbf{I_{MPP}}$, a perfect MPP operation can occur and the system has nearly $\boldsymbol{K_{pv}}$=100%.

3.2 European utilization& efficiency factors

Usually the actual PV systems operate at different insolation levels and considered nonlinear systems. Hence, performance parameters and factors (such as the efficiency, $\boldsymbol{K_{pv}}$ …etc) are nonlinear. In order to make a fair comparison of the

inverters under partial load conditions, the European factors are defined [20-22]. For example, the European efficiency is defined as:

$$\eta_{\mathrm{EU}} = 0.03\eta_{5\%} + 0.06\eta_{10\%} + 0.13\eta_{20\%} + 0.1\eta_{30\%} + 0.48\eta_{50\%} + 0.2\eta_{100\%} \quad (11)$$

By the same manner, the European $\boldsymbol{K_{pv}}$ is defined as [15]:

$$k_{\mathrm{pv}}\big|_{EU} = 0.03k_{\mathrm{pv}}\big|_{5\%} + 0.06k_{\mathrm{pv}}\big|_{10\%} + 0.13k_{\mathrm{pv}}\big|_{20\%} + 0.1k_{\mathrm{pv}}\big|_{30\%} + 0.48k_{\mathrm{pv}}\big|_{50\%} + 0.2k_{\mathrm{pv}}\big|_{100\%} \quad (12)$$

4. SIMULATION RESULTS

The The PV grid connected system with the conventional HERIC inverter, shown in Fig.2, is simulated using Matlab. The system parameters are given in Table [1]. The PV panel of the proposed system has the same power as the conventional one but rearranged to have the parameters given by Table [1].The inverter is as usual a current controlled inverter operating at unity power factor. The current controller was a PI controller. The PI controller generates the modulating signal for the traditional sine-triangle SPWM unit. In turn, the SPWM unit produces the gate signals for the H-bridge switches.

Table 1 System Parameters

	Parameters	Value
	PV SC current	16.35A
	PV OC voltage	533 V
Proposed	PV SC current	32.7A
Proposed	PV OC voltage	266 V
	Filter capacitance (C_f)	2nF
	Filter inductance (L_f)	1.8 mH
	Grid voltage	230V
	Grid frequency	50Hz
	Switching frequency	10KHz
	DC link capacitor	2000μF

While the gate signals for Q_5 and Q_6 are square waves synchronized to the grid voltage. The reference current of the current controller was the output of MPP tracking unit through a gain. The filter type was a symmetrical LCL, as recommended by [12]. The grid current, the PV current, the inverter voltage, and the earth leakage current of the simulated system, are shown in Fig. 7. The earth leakage current is 20mA less than the German VDE -0126 -1-1 standards [12]. Figure 8 shows the grid current, the PV current, the inverter voltage, and the earth leakage current of the proposed system. The PV current is constant at $\mathbf{I_{MPP}}$, which is 29.7A at this operating point, to insure true MPP operation. This issue forces the system to operate at a high utilization factor. The comparison of the utilization factor $\boldsymbol{K_{pv}}$ of both the conventional HERIC and proposed at different PV output power levels is shown in Fig. 9. The figure indicates that $\boldsymbol{K_{pv}}$ of the conventional HERIC is low (around 50%) as depicted by the previous analyses. If the current absorbed from the PV is set to $\mathbf{I_{MPP}}$, then $\boldsymbol{K_{pv}}$ must be 50%. As the MPP operation is vague, the PV current may take values apart from MPP condition, which demonstrates $\boldsymbol{K_{pv}}$ variations around 50%. It is also noted that the maximum output power from the conventional HERIC is limited to nearly half the PV power rating.

The calculated European $\boldsymbol{K_{pv}}$ for the proposed and the conventional HERIC topologieswere99.9% and 56% respectively. The efficiency comparison curves of the proposed and the conventional HERIC topologies are illustrated in Fig.10. Note that the presented efficiency diagram covers the total device losses and the output filter losses but it does not include the losses for the control circuit. It is clear that the efficiency difference between of the proposed and the conventional topology is very small. It also to be noted that the efficiency decays slightly as the output power increase. The reason behind this is the increase of the conduction losses with the increase of the output power. However, the switching losses are greatly affected by the switching frequency which is nearly constant at all power levels. In Fig. 9 and 10 the output power of the conventional HERIC system is limited to nearly half the PV rated power. European efficiency of the proposed and HERIC topologies are 95.5% and

96.6% respectively, which are calculated using equation (12).

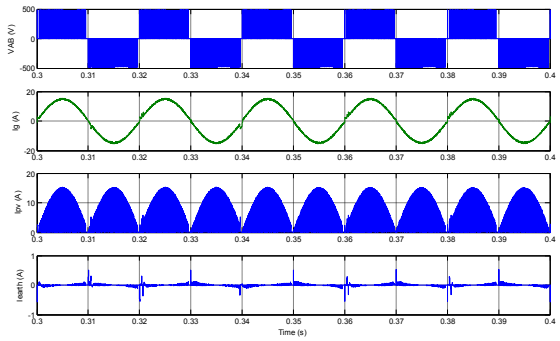

Fig. 7 The simulated inverter voltage, grid current, the PV current, and the earth leakage current of the conventional HERIC inverter.

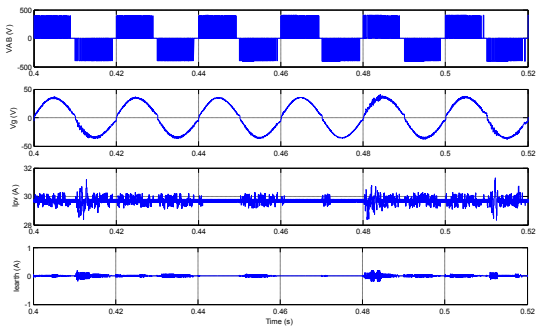

Fig. 8 The simulated inverter voltage, grid current, the PV current, and the earth leakage current of the proposed HERIC inverter.

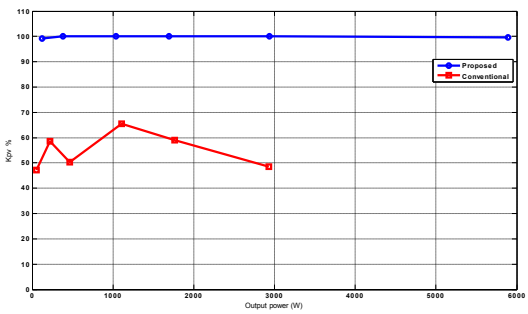

Fig. 9 Variations of K_{pv} with P_{pv} for the conventional and proposed systems.

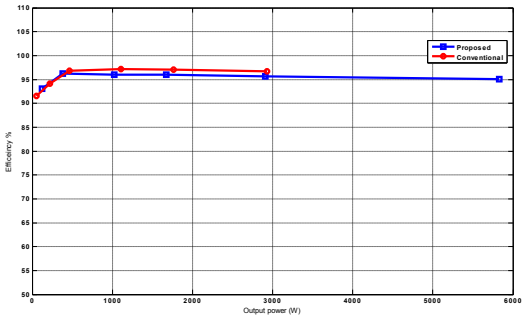

Fig. 10The efficiency comparison curves of the proposed topology and the conventional HERIC topology.

5. Conclusions

FOC In this paper, investigations of the utilization factor of the conventional HERIC transformerless grid connected inverter are carried out. Based on some reasonable assumptions, an expression for the utilization factor is derived. The result was surprising that the utilization factor of the conventional HERIC inverter is around 50%. Also, some problems related to the MPP operation of the PV with this inverter are discussed. It is also explained that MPP operation with is it vague and does not give actual maximum power extraction. An improved HERIC inverter system is proposed to elevate these problems. The simulation results shows that the proposed system has nearly 100% utilization factor and proofs MPP operation. However the overall efficiency of the new system is slightly less the conventional one.

References

[1] G . Parkinson . (2015, Jan 29). [Online]. Avail-able: http://cleantechnica.com/2015/01/29/solar-costs-will-fall-40-next-2-years-heres/.

[2] G . Parkinson . (2015, May 26). [Online]. Avail-able: http://cleantechnica.com/2015/05/26/solar-pv-costs-to-fall-another-25-per-cent-in-three-years/

[3] Li Zhang; Kai Sun; Yan Xing; Mu Xing, "Grid-Connected Photovoltaic Generation Plants, "IEEE Ind. Electronics Magazine, vol. 7, no.3, pp. 6-20, Sept. 2013.

[4] Trends in Photovoltaic Applications. Survey report of selected IEA countries between 1992 and 2004, Photovoltaic Power Systems Program . Report IEA-PVPS T1-14: 2005 , 2005

[5] Eugenio Gubı´a, Pablo Sanchis, Alfredo Ursu´a, Jesu´ sLo´pez and Luis Marroyo, "Ground Currents in Single-phase Transformerless Photovoltaic Systems," Prog. Photovolt: Res. Appl.2007; 15:629–650.

[6] Li Zhang; Kai Sun; Yan Xing; Mu Xing, "H6 Transformerless Full-Bridge PV Grid-Tied Inverters," Power Electronics, IEEE Transactions on , vol.29, no.3, pp.1229-1238, March 2014 doi: 10.1109/TPEL.2013.2260178.

[7] R. Gonzalez, J. Lopez, P. Sanchis, and L. Marroyo, "Transformerless inverter for single-phase photovoltaic systems," IEEE Trans. Power Electron., vol. 22, no. 2, pp. 693–697, Mar. 2007.

[8] H. Xiao, S. Xie, "Leakage current analytical model and application in single-phase transformerless photovoltaic grid-connected inverter," IEEE Trans. ElectromagnCompat., vol. 52, no. 4, pp. 902–913, Nov. 2010.

[9] W. N. Mohan, T. Undeland, and W. P. Robbins , Power Electronics: Converters, Applications, and Design. New York: Wiley, 2003.

[10] Wuhua Li, Yunjie Gu, Haoze Luo, Wenfeng Cui, Xiangning He, and Changliang Xia, "Topology Review and Derivation Methodology of Single Phase Transformerless Photovoltaic Inverters for Leakage Current Suppression," IEEE Trans. Ind. Elec., vol. 41, no. 5, pp. 1292-1306, 2015.

[11] [11]J. M. A. Myrzik, M. Calais, "String and module integrated inverters for single-phase grid connected photovoltaic systems - a review, " in Proc. IEEE Power Tech Conference Proceedings, 2003.

[12] [12] Kerekes T. Analysis and modeling of transformerless photovoltaic inverter systems. (PhD). Aalborg University, The Faculty of Engineering and Science, Department of Energy Technology; 2009

[13] O. Lopez, F. D. Freijedo, A. G. Yepes, P. Fernandez-Comesana, J. Malvar, R. Teodorescu, and J. Doval-Gandoy, "Eliminating ground current in a transformerless photovoltaic application," IEEE Trans. On Energy Conversion, vol. 25, no. 1, pp. 140–147, Mar. 2010.

[14] S. Heribert, S. Christoph, and K. Jurgen, "Inverter for transforming a DC voltage into an AC current or an AC voltage," Europe Patent 1 369 985(A2), May 13, 2003.

[15] S. B. Kjaer, J. K. Pedersen and F. Blaabjerg, "A review of single-phase grid-connected inverters for photovoltaic modules," IEEE Trans. Ind. Appl., vol. 41, no. 5, pp. 1292-1306, 2005.

[16] Haibing Hu, SouhibHarb, Nasser Kutkut, IssaBatarseh, Z. John Shen "Power Decoupling Techniques for Micro-inverters in PV Systems-a Review" Energy Conversion Congress and Exposition (ECCE), 2010 IEEE, Atlanta, GA,12-16 Sept., 2010, pp.3235 – 3240.

[17] Q. Li, P. Wolfs, "A Review of the Single Phase Photovoltaic Module Integrated Converter Topologies with Three Different DC Link Configurations", IEEE Trans. on Power Electronics, VOL. 23, NO. 3,MAY 2008.pp.1320-1333.

[18] S. Xing et al. (eds.),Unifying Electrical Engineering and Electronics Engineering , Lecture Notes in Electrical Engineering 238, DOI 10.1007/978-1-4614-4981-272, Springer Science Business Media New York 2014

[19] Søren Bækhøj Kjær , "Evaluation of the "Hill Climbing" and the "Incremental Conductance" Maximum Power Point Trackers for Photovoltaic Power Systems," IEEE Tran. on Energy Conv., Vol. 27,no. 4, pp. 922-929, Dec. 2012.

[20] H. Haeberlin, "Evolution of inverters for grid connected PV-systems from 1989 to 2000, " in Proc. 17th Eur. Photovoltaic Solar Energy Conf., Munich, Germany, Oct. 22–26, 2001, pp. 426–430.

[21] Maaspaliza Azri, Nasrudin Abd. Rahim & Wahidah Abd. Halim, "Overview of Single-phase Grid-connected Photovoltaic Systems" Electric Power Components and Systems,vol. 43, issue 12, July 2015, pp. 1352-1363.

[22] Yongheng Yang, and Frede Blaabjerg, "A Highly Efficient Single-phase Transformerless H-bridge Inverter for Reducing Leakage Ground Current in Photovoltaic Grid-connected System" Electric Power Components and Systems, vol. 43, issue 8-10, June 2015, pp. 928-938.